ORIGINAL ARTICLE

High-resolution imaging of human atherosclerotic carotid plaques with micro^{18}F-FDG PET scanning exploring plaque vulnerability

Marleen G. Masteling, MSc,[a] Clark J. Zeebregts, MD, PhD,[b,c]
René A. Tio, MD, PhD,[c,d] Jan-Cees Breek, MD, PhD,[e] Uwe J. F. Tietge, PhD,[f]
Jan Freark de Boer, BSc,[f] Andor W. J. M. Glaudemans, MD,[g]
Rudi A. J. O. Dierckx, MD, PhD,[g] Hendrikus H. Boersma, PharmD, PhD,[c,g,h] and
Riemer H. J. A. Slart, MD, PhD[c,g]

Aims. **FDG-PET can be used to identify vulnerable plaques in atherosclerotic disease. Clinical FDG-PET camera systems are restricted in terms of resolution for the visualization of detailed inflammation patterns in smaller vascular structures. The aim of the study is to evaluate the possible added value of a high-resolution microPET system in excised carotid plaques using FDG.**

Methods and Results. **In this study, 17 patients with planned carotid endarterectomy were included. Excised plaques were incubated in FDG and subsequently imaged with microPET. Macrophage presence in plaques was evaluated semi-quantitatively by immunohistochemistry. Plaque calcification was assessed additionally with CT and correlated to FDG uptake. Finally, FDG uptake and macrophage infiltration were compared with patient symptomatology. Heterogeneous distributions and variable intensities of FDG uptake were found within the plaques. A positive correlation between the distribution of macrophages and the FDG uptake ($r = 0.68$, $P < .01$) was found. A negative correlation was found between areas of calcifications and FDG uptake ($r = -0.84$, $P < .001$). Ratio FDG$_{max}$ values as well as degree of CD68 accumulation were significantly higher in CVA patients compared with TIA or amaurosis fugax patients ($P < .05$) and CVA patients compared with asymptomatic patients ($P < .05$).**

Conclusion. **This ex vivo study demonstrates that excised carotid plaques can be visualized in detail using FDG microPET. Enhancement of clinical PET/CT resolution for similar imaging results in patients is needed. (J Nucl Cardiol 2011;18:1066–75.)**

Key Words: Atherosclerosis · carotid artery · FDG · microPET · vulnerable plaque

doi:10.1007/s12350-011-9460-2

INTRODUCTION

Rupture of carotid atherosclerotic plaques and subsequent formation of thrombi or emboli are currently recognized as the primary cause of acute cerebrovascular disease.[1] The number of cerebrovascular events can be reduced by surgical removal of the stenosed plaque in the carotid artery. Currently, patients are selected for carotid endarterectomy (CEA) based on symptomatology and degree of stenosis.[2]

Conventional imaging of luminal stenosis can be used to identify plaque vulnerability, but lack of standardized quantifiable duplex, magnetic resonance imaging (MRI)/magnetic resonance angiography (MRA), or radiographic criteria for plaque instability limit their

reliability. Moreover, non-stenotic vulnerable plaques may also be prone to rupture, whereas stenosing stable lesions may remain stable and asymptomatic.[3] Plaque biology rather than degree of stenosis determines the risk of acute cerebrovascular events. Inflammation plays an essential role in the pathophysiology of atherosclerosis.[4] A high prevalence of macrophage-rich plaques is found in patient groups with acute cerebrovascular symptoms, and markers of macrophage activation are more abundant in ruptured plaques. In addition, macrophage infiltration is one important cause of plaque instability.[5]

Several studies have shown that [^{18}F]-fluorodeoxy-glucose (FDG) accumulates in plaques with high macrophage density; however, this was performed on clinical PET cameras with relative low resolution.[6-11] Therefore, FDG positron emission tomography/computed tomography (PET/CT) has emerged as a non-invasive imaging modality able to predict the susceptibility of plaques toward rupture on the patients' group level. FDG-PET/(CT) studies have shown significantly higher FDG uptake in symptomatic plaques compared to asymptomatic plaques and healthy controls.[12-17] Despite these promising results, it is hard to select high risk patients based on FDG-PET/(CT) results, conceivably due to limited clinical PET camera resolution and the lack of validated clinical endpoint trials. Clinically, FDG uptake in vulnerable plaques is difficult to detect. The spatial resolution of a clinical PET scanner ranges 5-10 mm and smaller FDG avid atherosclerotic plaques will therefore be missed. High-resolution microPET systems with a spatial resolution of as low as 1 mm are able to visualize smaller metabolically active lesions.[18] Furthermore, there is evidence that FDG-uptake is correlated to the extent of macrophage infiltration within a plaque using material obtained from clinical patients.[19,20]

The aim of this study is to evaluate whether enhanced FDG uptake on high-resolution microPET correlates with macrophage infiltration and, therefore, with plaque instability and with neurological symptom status. Also, the necessity for resolution enhancement in currently available clinical PET/CT is evaluated.

METHODS

Patients

Twenty consecutive patients with significant carotid artery stenosis (70%-99%) who underwent CEA at the Department of Surgery (Division of Vascular Surgery) in the University Medical Center Groningen or the Martini Hospital in Groningen participated in this study. The degree of stenosis and basic morphologic features of the plaque were evaluated by duplex ultrasound. Patient selection and operative technique were based on the recommendations as published by NASCET

and ECST.[21,22] Out of twenty patients, three patients were excluded from further analysis as their material was primarily used for validation purposes in a pilot study. Of the remaining seventeen patients, three patients had a conventional FDG-PET/computed tomography angiography (CTA) 1 week before CEA. Information about the clinical status was collected from the hospital information system and included medical history, diagnosis, treatment, medication, symptoms, smoking, and risk factors.

Relevant baseline characteristics of the 17 patients are summarized in Table 1. The median age was 71 years (range 45-82), 12 patients (71%) were male. The main risk factors were lipid disorder in 9 (53%), hypertension in 12 (71%), smoking in 10 (59%), and diabetes mellitus in 2 (12%) patients. Eligibility for CEA was determined based on the presence of a stenosis of 70%-99%, and in one patient (patient 2) with a degree of stenosis of 50%-70% due to ulcerative plaque formation on ultrasound.

This study was approved by the Institutional Ethics Review Boards of both hospitals and all included patients gave written informed consent before inclusion in the study.

Plaque Preparation

CEA was performed under general anesthesia using standard techniques; plaques were removed gently and transported in phosphate-buffered saline (PBS). The plaques were then directly incubated in approximately 100 MBq FDG for 60 minutes by 37°C. After incubation, resected plaques were flushed with PBS and were subsequently stored in a humid environment during the microPET imaging procedure to prevent dehydration. Immediately after the imaging procedure, carotid plaque material was sliced transversely in 3-5 slides. Careful attention was given to orientation and slice origin (common carotid artery, bifurcation, and internal carotid artery), and this was marked and noted. Then, the slices were immediately fixed in formalin for 48 hours and subsequently embedded in paraffin.

Image Acquisition MicroPET/CT, Reconstruction and Data Analysis

After incubation with FDG, 17 atherosclerotic plaques were imaged using a microPET scanner (micro PET Focus 220, Siemens/Concorde). A list-mode protocol was used (60 minutes). A transmission scan of 15 minutes with a radioactive point source was obtained for the correction of attenuation by tissue. Acquisition data were reconstructed using iterative reconstruction and segmented attenuation. PET image analyses were performed using standard software (AsiPro VM 6.2.5.0; Siemens/Concorde and Siemens Inveon Research *Workplace* (IRW) (Siemens Medical Systems, Knoxville, Tennessee, USA).

Seven atherosclerotic plaques were also imaged using a microCT scanner (Siemens Imtek MicroCAT II, Siemens Medical Systems, Knoxville, Tennessee, USA). The CT system was calibrated to acquire 512 projections at 55 kVp with a 57×85 mm^2 field of view (FOV). The exposure time was

Table 1. Individual patient data, risk factors and diagnostic data

Patient no.	Gender	Age (years)	Symptoms	Statins	Hyperlipidemia	Hypertension	Smoking	Degree of stenosis (%)*	Ratio FDG max†	CD68‡
1	M	74	R CVA	4	3	3	0	80-99	3.53	2.50
2	M	78	R TIA	2	3	1	1	50-70	3.04	2.50
3	F	72	L TIA	2	-	0	0	80-99	4.70	2.00
4	M	67	R A. fugax	2	0	0	0	70-99	3.44	1.00
5	F	81	R TIA	2	0	2	2	70-99	1.78	-
6	M	68	L TIA	0	3	1	2	70-99	4.19	2.50
7	M	72	R CVA	2	0	1	0	80-99	4.79	2.60
8	F	72	R TIA	1	0	1	0	70-99	4.19	0.00
9	M	71	L CVA	3	0	0	0	80-99	4.41	2.20
10	M	70	L A. fugax	2	3	0	0	70-99	1.97	0.67
11	M	82	L CVA	2	3	3	2	80-99	4.86	2.67
12	F	67	R TIA	2	3	3	2	70-99	4.13	2.40
13	M	77	R TIA	0	0	1	2	80-99	4.77	2.50
14	F	45	R CVA	0	0	2	2	80-99	8.66	2.67
15	M	61	L-	4	3	3	1	70-99	3.88	0.60
16	M	69	R CVA	1	3	0	2	80-99	4.56	3.50
17	M	60	R-	2	3	1	1	80-99	2.50	2.00

Statins: 0 = none, 1 = simvastatin 20 mg, 2 = simvastatin 40 mg, 3 = atorvastatin 20 mg, 4 = atorvastatin 40 mg; hyperlipidemia: 0 = cholesterol and triglycerides within normal range for age, 3 = requires dietary and drug control; hypertension: 0 = none, 1 = controlled with single drug, 2 = controlled with 2 drugs, 3 = requires more than 2 drugs or uncontrolled; smoking: 0 = none, or none for last 10 years, 1 = currently none, but smoked in last 10 years, 2 = current (includes abstinence <1 year).
R, Right side carotid stenosis; L, left side carotid stenosis; A. fugax, amaurosis fugax; TIA, transient ischemic attack; CVA, cerebrovascular accident; absent specifications represent asymptomatic patients.
* Degree of stenosis: carotid artery stenosis determined by duplex flow analysis.
† Ratio FDGmax: highest FDG uptake corrected for background FDG uptake.
‡ CD68: CD68 positive cells (macrophages) were semi-quantitatively scored; the average score is presented.

1050 seconds and binning 4 (4 × 4 pixels = 1 pixel) was used. After the microPET scanning was complete, the plaque was turned axially and centered within the CT detector ring, to maintain the same stereotactic position. Spatial resolution was 37 μm isotropic for CT and <1.3 mm at the center FOV for PET imaging. The microPET and CT images were fused using a software module in IRW. The plaque remained in the same position on the bed for both PET and CT acquisitions and the relative positions of the FOVs of the PET and CT were known. A software module was used for fusion and co-registration of PET and CT data, but if needed partly corrected manually. Fused images were analyzed by placing volumes of interest around the calcified areas. PET images were analyzed and categorized by one observer as follows: a region of interest (ROI) was drawn around the whole plaque and mean FDG uptake and maximum uptake were determined in MBq/mL and corrected for background activity (lowest uptake region of the remaining plaque). RatioFDG$_{max}$ was calculated as maximum FDG uptake (hot spot) divided by background activity. For each section within the sliced plaque, the highest FDG uptake value and the mean FDG uptake were determined by inserting ROIs. RatioFDG$_{overall}$ was calculated by dividing the mean FDG uptake (whole slide) by the background activity. In addition, the volume of calcification, as recognized as less variable than the Agatston method,[23] within a plaque was assessed by microCT and compared with maximum FDG uptake of the corresponding plaque.

Reagents and Immunohistochemistry

FDG was produced at our institute according to the Hamacher method (nucleophilic fluorination reaction followed by deprotection).[24] Sections (3 μm) of routinely processed, formalin-fixed, paraffin-embedded tissues were deparaffinized and rehydrated. Endogenous peroxidase activity was blocked using 0.3% H$_2$O$_2$ in PBS for 30 minutes at room temperature. The sections were pre-treated with microwave antigen retrieval methods using 0.01 M citric acid (pH 6.0) in distilled water. Subsequently, nonspecific antigenic protein binding was blocked with 4% normal goat serum in PBS for 20 minutes. The degree of inflammation was evaluated by CD 68 immunostaining for macrophages. Sections were incubated with mouse anti-CD68 monoclonal antibody (clone KP1, Abcam, Cambridge, UK) at a 1:100 dilution in PBS containing 1% bovine serum albumin (BSA) for 2 hours at room temperature. After washing, the sections were incubated with an Alexa-594
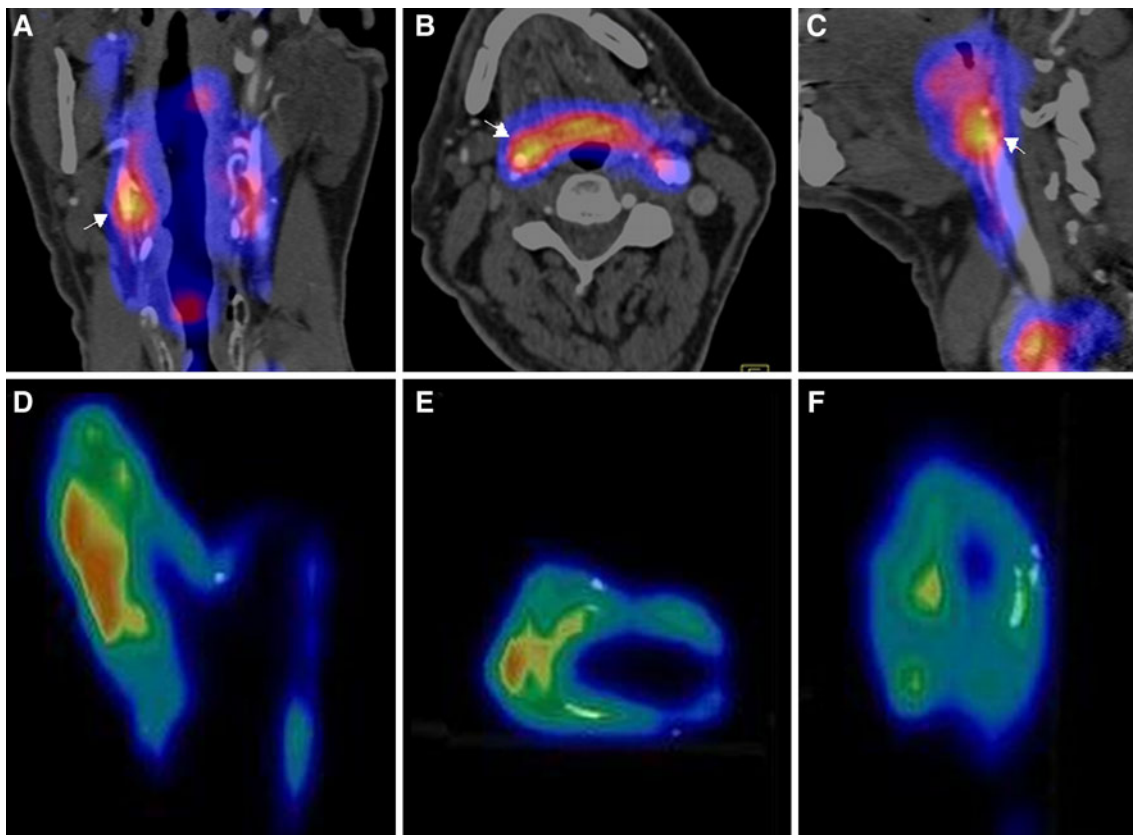

Figure 1. Clinical PET image with coronal (**A**), transverse (**B**), and sagittal (**C**) plane slices of a patient showing FDG uptake in the affected right carotid artery (*arrows*). Coronal (**D**), transverse (**E**), and sagittal plane (**F**) of corresponding μPET images of the same patient showing also patchy FDG uptake and calcified areas (*white* depositions).

conjugated goat anti-mouse antibody (1:500 dilution in PBS/ 1%BSA) for 30 minutes at room temperature. 4′,6-Diamidino-2-phenylindole (DAPI, Molecular Probes, Eugene, Oregon, USA) was added to this solution (1:2000) to visualize the nuclei. Negative staining control sections received the same treatment, except that the first antibody was omitted. Sections were washed with water and subsequently mounted in fluorescent-mounting medium (Dako, Glostrup, Denmark). Stained sections were evaluated using fluorescence microscopy (Leica DM LB, Rijswijk, the Netherlands) with standard excitation filters; DAPI, FITC, and TRITC.

The degree of inflammation in obtained histological specimens was compared with the mean FDG values, corrected for background FDG uptake in the corresponding ROI (ratio-FDG$_{overall}$). The 17 obtained plaque specimens yielded 66 plaque sections (4 ± 1 sections/patient) after slicing.

Analysis of Immunohistochemical Staining

CD68 staining was analyzed and categorized independently by two observers. Inter-observer variability was excellent, with an agreement of 100%. According to the inhomogeneous and accentuated distribution of histopathologic patterns, semiquantitative analyses were performed to describe the predominant histologic characteristics in the entire sample. The semiquantitative analysis was used because it is a widely used method and accompanied with a high reproducibility.[25] The careful attention that was given to orientation and slice origin (common carotid artery, bifurcation, and internal carotid artery) of the sliced plaque by demarcation was compared with the microPET and microCT images.

Specimens were evaluated by using a score of: I = absent or minor staining in the entire slide; II = mild; III = moderate; IV = extensive. In addition, regional clustered macrophages were scored as follows: 0 = no clustered cells (<10%); I = few clustered cells (10%-25%); II = small area of clustered cells (25%-50%); III = moderate area of clustered cells (50%-75%) IV = extensive area of clustered cells (>75% macrophages/ surface). We compared FDG uptake and macrophage infiltration of endarterectomized plaques originating from asymptomatic and symptomatic patients.

Statistical Analysis

Data were analyzed using SPSS for Windows version 16.02. Descriptive statistics are expressed as mean ± SD (continuous variables), except time from CEA to FDG incubation and FDG incubation time which are presented as median, or as percentages to reflect patient details (dichotomous measures). Univariate correlations were calculated using Spearman's rank test.

Simple linear regression analysis was performed to explore the associations between FDG variables (outcome variables) and the biomarkers calcification and CD68 (explanatory variables) Simple linear regression analysis was also performed between CD68 (outcome variables) and the explanatory variables biomarkers and calcification. Linear regression analysis was corrected for multiple segments per patients. Non-parametric tests (Kruskal-Wallis and Mann-Whitney U) were used to describe differences in subgroups that had a skewed distribution. Values of $P < .05$ were considered as significant.

RESULTS

There were clear differences between the microPET/ CT images of the CEA specimen of a representative patient compared to a corresponding clinical PET/CT images obtained in the same patient (Figure 1). Visually, microPET/CT images reveal patchy FDG uptake within the plaques. FDG microPET images of this patient showed FDG uptake in the plaque more in detail compared with the clinical PET scan.

The relation between FDG uptake and macrophage number is plotted in Figure 2. A significant correlation was found between ratioFDG$_{overall}$ and histological inflammation [macrophage infiltration in the entire slice (CD68 overall)] ($r = +0.68$, $P < .001$; Figure 2). Concordant with this observation, ratioFDG$_{max}$ values in the ROI were also significantly associated with inflammation (CD68 overall) ($r = +0.32$, $P < .001$).

Figure 3 shows a plaque with cold and hot areas, as defined by FDG uptake, confirmed by intense macrophage infiltration in the hot area and no macrophage infiltration in the cold area. The calcification level was inversely correlated with ratioFDG$_{max}$ ($r = -0.84$, $P < .001$), meaning absent or minimal plaque calcification was associated with extensive FDG uptake and dense plaque calcification was associated with little uptake. This inverse correlation could also be observed for macrophages inflammation (mean CD68 overall) and
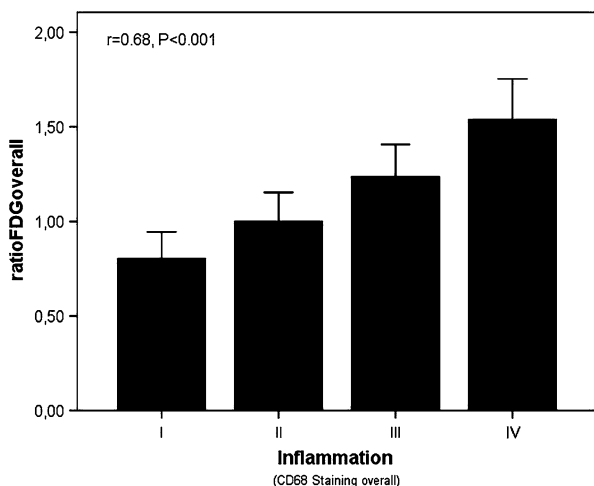

Figure 2. Mean maximum FDG uptake corrected for background activity (ratioFDG$_{overall}$) is significantly correlated with the degree of inflammation assessed as semi-quantitative CD 68 expression scored on the entire slide in the corresponding plaque section ($r = +0.68$, $P < .001$).
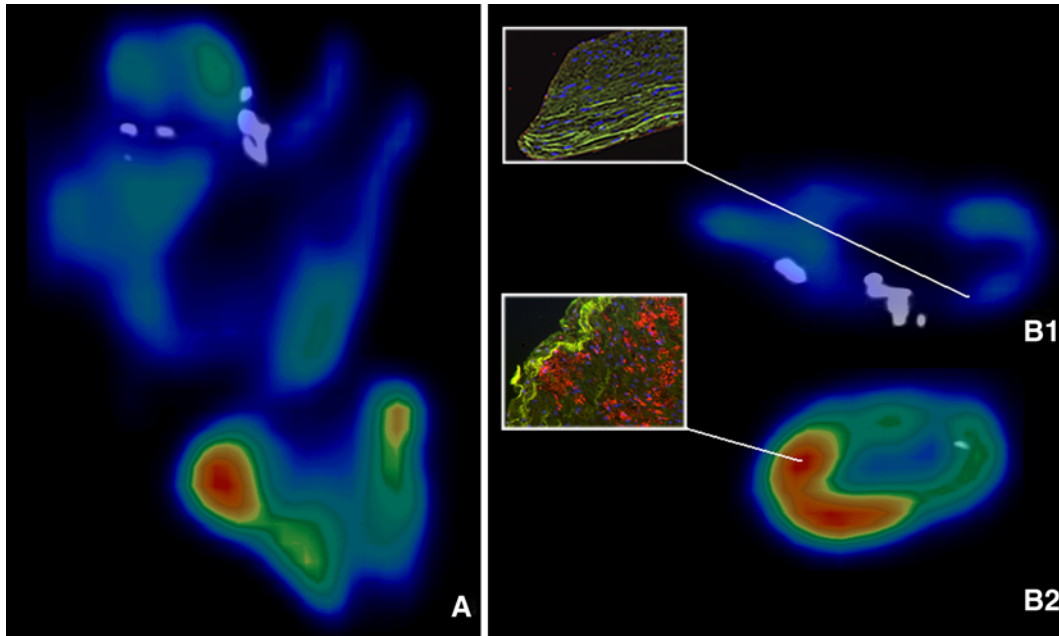
Figure 3. FDG microPET/CT image of an ex vivo carotid plaque in the coronal plane (**A**), transverse plane (**B**) and the corresponding histological results. An overview of the plaque with low FDG uptake in the cranial part of the plaque and with high FDG uptake in the more caudal part of the plaque (**A**). Difference in FDG uptake in a transverse section of the cranial part of the plaque compared to the FDG uptake in a transverse section of the caudal part of the plaque (**B1**, **B2**). CD68 macrophage staining showing abundant inflammation (side view frame **B2**) in accordance with FDG uptake values (**B2**). Macrophages could not be observed in the histological section that corresponds with **B1** (side view frame **B1**). Dapi stained nuclei are visualized (*blue*). The *green* auto-fluorescence allows an assessment of tissue structure.
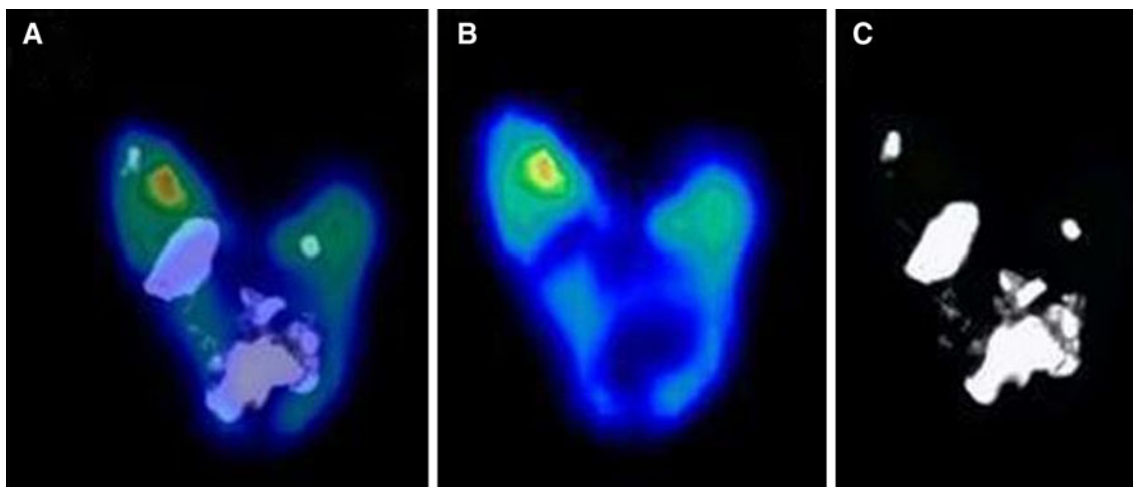

Figure 4. Fused coronal FDG microPET/CT image of a heavily calcified carotid plaque (**A**). Coronal [18]FDG microPET image (**B**). *Blue* low FDG uptake, *red* high FDG uptake. Coronal CT image of the same heavily calcified plaque (**C**).

total calcium volume within plaques ($r = -0.79$, $P < .05$).

Figure 4 displays the microCT image and micro-PET image of the same plaque, for which the calcified area showed no evident FDG uptake. The mean ratio-FDG_{max} was 4.08 ± 1.53 (range 1.78-8.66). In addition, the mean of the average macrophage (CD68) clustering score was 2.02 ± 0.95 (range 0.00-3.50).
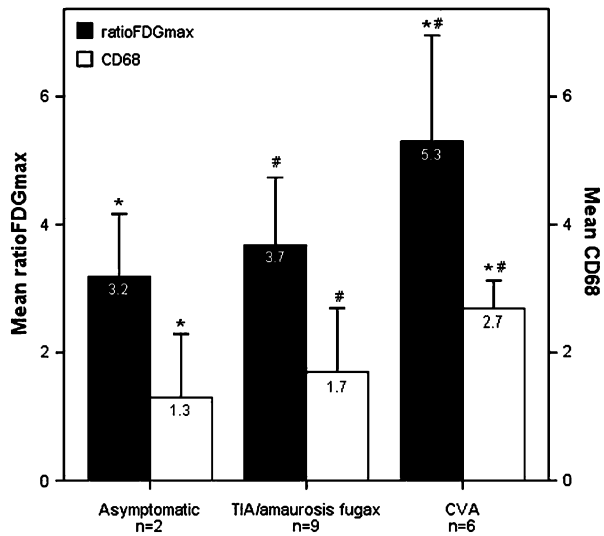
Figure 5. Mean maximum FDG microPET uptake corrected for background activity (ratio FDG_{max}) ± SD (*black bars*) and mean average concentration of clustered macrophages (CD68) ± SD (*white bars*) in specimens obtained in asymptomatic, TIA/amaurosis fugax and CVA patients. The graph depicts the relation between $ratioFDG_{max}$, inflammation and patient symptoms. CVA patients showed significant increased maximum FDG uptake and CD68 infiltration compared with TIA/amaurosis fugax and asymptomatic patients (*$P < .05$ CVA vs asymptomatic patients, #$P < .05$ CVA vs TIA/amaurosis fugax patients). There was no statistically difference in $ratioFDG_{max}$ or CD68 between asymptomatic and TIA/amaurosis fugax patients. *TIA*, transient ischemic attack; *CVA*, cerebrovascular accident.

The mean $ratioFDG_{max}$ was 4.08 ± 1.53 (range 1.78-8.66). In addition, the mean of the average macrophage (CD68) clustering score was 2.02 ± 0.95 (range 0.00-3.50). There was a trend toward higher FDG uptake and macrophage accumulation in patients displaying more severe symptomatology, when divided into three groups of increasing severity of symptomatology: asymptomatic patients, patients with TIA or amaurosis fugax, and patients with CVA, respectively (Figure 5). Figure 5 displays $ratioFDG_{max}$ values and CD68 staining scores for different patient symptoms. Ratio FDG_{max} values as well as the degree of CD68 accumulation were significantly higher in CVA patients compared with TIA or amaurosis fugax patients ($P < .05$) and CVA patients compared with asymptomatic patients ($P < .05$). A comparison between patients with TIA or amaurosis fugax and asymptomatic patients did not reach significance.

DISCUSSION

This study demonstrates for the first time proof of concept to perform detailed ex vivo visualization of carotid atherosclerotic plaques after endarterectomy

using a microPET camera system with a spatial resolution of approximately 1 mm. FDG uptake correlated well with macrophage infiltration determined by immunohistochemistry of CD68, an established surrogate marker for increased local inflammation and decrease plaque stability. Finally, our data also point toward a potential link between FDG uptake and actual patient symptoms, further stressing the usefulness of developing PET systems with improved resolution for clinical application.

Currently, there is a demand for novel non-invasive screening procedures to detect potentially life-threatening vulnerable plaques.[26] FDG-PET/CT is of interest, since FDG accumulates in activated macrophages which are considered to be causally related to vulnerable plaque rupture. Moreover, in contrast to many other PET-tracers, it is widely available. Therefore, FDG-PET/CT represents a promising tool for better selection of patients for CEA. However, the small differences in ranges for TBR found between the different patient groups, which is in accordance with the results of previous studies[12,14,20,27] reveal that it is yet not possible to use FDG-PET/CT as a diagnostic tool. At this moment there is, therefore, no imaging method available that has reached the level of clinical decision-making.

Animal atherosclerotic plaque imaging studies revealed strong correlations between FDG uptake and macrophage content.[7,11,28] Interestingly, Davies et al.[28] demonstrated that macrophage content and ex vivo FDG-microPET uptake correlated well in a rabbit model ($r = 0.95$, $P < .001$), while in vivo quantification did not support this finding ($r = 0.16$, $P = .57$). When the intended target is smaller than the spatial resolution, partial volume errors (PVE) will arise. Then, surrounding tissue may be responsible for the observed discrepancy. Furthermore, Tawakol et al.[11] showed in a rabbit model that the correlation of FDG uptake and macrophages was lower when the controls were left out ($r = 0.73$ vs $r = 0.93$). This is of interest since there is a need for patient selection to distinguish stable from vulnerable plaques, instead of atherosclerotic arteries from healthy arteries. Macrophages have a glucose turnover at baseline which is 5- to 20-fold higher compared to surrounding tissue. Moreover, glucose utilization can increase 50-fold further when macrophages are activated.[29] Therefore, it should be feasible to visualize macrophages containing tissue with clear demarcation. However, atherosclerotic plaques consist for a substantial part of necrotic tissue. Thus, more sophisticated PET cameras need to be developed to detect infiltrating macrophages using FDG and overcome PVE. Another possibility may be the use of technetium labeled annexin A5, an apoptosis marker that can detect carotid plaques with a higher spatial

resolution.[30] A plausible explanation might be that the phosphatidyl serine (PS) binding protein annexin A5 is far more specific than FDG which in principle accumulates in all cells, and is therefore more hampered by PVE. Annexin A5 will not only attach to PS-expressing macrophages, but also to PS-containing blood platelets which are abundant in plaque tissue. In contrast, FDG might also accumulate non-specifically in surrounding gland tissue thereby mimicking carotid plaque uptake. It could therefore be an option to explore the properties of more specific ligands for the assessment of the atherosclerotic plaque. The problem with novel tracers, however, is their availability, which makes it more difficult to compete with FDG.

In contrast to clinical PET scanning, microPET scanning with FDG revealed a heterogeneous accumulation pattern (Figure 1), including high intensity contrasts within the plaque with a clear demarcation. This is of great clinical value since not only the presence of macrophages but also their location in tissue are key factors in determining risk.

It has been well established that FDG accumulates at sites of atherosclerosis in humans. However, the correlation of in vivo FDG uptake and macrophages has only been assessed by Graebe et al.,[27] Font et al.,[31] and Tawakol et al.[32] To our knowledge our study is the first to correlate FDG uptake in endarterectomized plaques and macrophage content ex vivo, using microPET scanning. The correlation we found between macrophages and FDG uptake was in the same range as the correlation found by Tawakol et al.[32] ($r = 0.70$, $P < .001$) using a clinical PET scanner. We sectioned the plaques similar to Tawakol et al. and discovered large differences in macrophage content between different section levels within a given plaque and large differences in FDG uptake in general. However in our study the camera resolution matched the thickness immunohistochemistry slices well than in this previous study. A possible explanation for this observation could be the inclusion of surrounding tissue that interferes with the SUV value estimation as well as the differences in clinical camera system resolution (5-10 mm) combined with the used section slices (3 mm).[32]

Sheikine and Akram[20] suggested in a recent review that there is a gap to bridge between FDG uptake and histological findings. Therefore, we compared FDG uptake and macrophage infiltration of endarterectomized plaques originating from asymptomatic and symptomatic patients. FDG uptake (ratioFDG$_{max}$) and macrophage content (CD68) were not only highly correlated but also showed similar patterns with respect to clinical outcome. The difference between CVA and TIA patients reached significance for ratioFDG$_{max}$ ($P < .05$). Our findings illustrate that FDG-PET may

have potential for clinical decision-making, and underscore the clear need for more research and sophisticated PET cameras.

The studies on FDG accumulation at sites of calcification thus far revealed conflicting results.[9,10,20,33-38] FDG-avid lesions and calcified lesions at the same vascular location are uncommon as mentioned in previous studies.[9,10,33-35,37] Our findings are in accordance with these previous findings. Moreover, we also showed that there is a high negative correlation between calcification and FDG ($r = -0.84$, $P < .01$). The excellent spatial resolution of both microPET (~ 1 mm) and μCT (37 μm) compared to the clinical PET camera system (5-8 mm) or clinical CT (1 mm) might be an explanation for the higher negative correlation as observed in our study compared to the study of Rudd et al. ($r = -0.42$, $P = .03$).[9] Laitinen et al.,[36] in contrast, detected non-specific binding to calcified structures using in vitro autoradiography of FDG in calcified human arteries. They ascribed this inconsistency to the spatial resolution of clinical CT scans compared to their ability to visualize small calcified structures. Use of microPET and microCT provided an excellent visualization of small calcified structures (Figure 4). The FDG uptake seen at the border of calcification is probably due to partial volume effects. Therefore, it is conceivable that the FDG uptake in calcified structures noted in other studies is an artifact of the imaging technique related to insufficient resolution.

It is suggested that FDG-avid atherosclerosis is a precursor, followed by persistent calcification at the same site.[14,39] Paulmier et al.[40] demonstrated that arterial calcifications are closely related to old cardiovascular events and do not point out progressive plaque formation, in contrast to FDG-avid lesions. Our results thereby emphasize that plaque calcification and FDG-avid lesions are different pathophysiologic entities.

The primary limitation of this study is that carotid plaques are exposed to ischemia (transport and incubation time), which could potentially interfere with FDG uptake. Despite this limitation, we observed a strong correlation between the degree of FDG uptake and the amount of macrophages present in the tissue. Therefore, we assume that FDG uptake is not substantially altered by ischemia. In addition this proof of concept study comprises a small study population with relatively small subgroups, in particular regarding asymptomatic patients. However, our results still point out the clear clinical need for PET-systems with enhanced resolution.

In conclusion, we demonstrate that carotid atherosclerotic plaques can be visualized ex vivo after CEA with great detail using a high-resolution microPET camera system revealing potentially important information that can be easily missed with clinical PET

camera systems. Interestingly, FDG uptake correlated strongly with macrophage infiltration, indicating that enhanced resolution PET imaging would be particularly useful for the detection of vulnerable and thereby rupture-prone plaque-areas. Our results demonstrate the clear need for novel clinical PET/CT cameras with high resolution for optimal vascular imaging using the readily available FDG.

Conflict of interest

The authors declare that they have no conflict of interest.

Open Access

This article is distributed under the terms of the Creative Commons Attribution Noncommercial License which permits any noncommercial use, distribution, and reproduction in any medium, provided the original author(s) and source are credited.

References

1. Izquierdo-Garcia D, Davies JR, Graves MJ, Rudd JH, Gillard JH, Weissberg PL, et al. Comparison of methods for magnetic resonance-guided [18-F]fluorodeoxyglucose positron emission tomography in human carotid arteries: Reproducibility, partial volume correction, and correlation between methods. Stroke 2009;40:86-93.
2. Chaturvedi S, Bruno A, Feasby T, Holloway R, Benavente O, Cohen SN, et al. Carotid endarterectomy—an evidence-based review: Report of the Therapeutics and Technology Assessment Subcommittee of the American Academy of Neurology. Neurology 2005;65:794-801.
3. Wallis de Vries BM, van Dam GM, Tio RA, Hillebrands JL, Slart RH, Zeebregts CJ. Current imaging modalities to visualize vulnerability within the atherosclerotic carotid plaque. J Vasc Surg 2008;48:1620-9.
4. Chen W, Bural GG, Torigian DA, Rader DJ, Alavi A. Emerging role of FDG-PET/CT in assessing atherosclerosis in large arteries. Eur J Nucl Med Mol Imaging 2009;36:144-51.
5. Jander S, Sitzer M, Schumann R, Schroeter M, Siebler M, Steinmetz H, et al. Inflammation in high-grade carotid stenosis: A possible role for macrophages and T cells in plaque destabilization. Stroke 1998;29:1625-30.
6. Fifer KM, Qadir S, Subramanian S, Vijayakumar J, Figueroa AL, Truong QA, et al. Positron emission tomography measurement of periodontal (18)f-fluorodeoxyglucose uptake is associated with histologically determined carotid plaque inflammation. J Am Coll Cardiol 2011;57:971-6.
7. Ogawa M, Ishino S, Mukai T, Asano D, Teramoto N, Watabe H, et al. (18)F-FDG accumulation in atherosclerotic plaques: Immunohistochemical and PET imaging study. J Nucl Med 2004;45:1245-50.
8. Rudd JH, Warburton EA, Fryer TD, Jones HA, Clark JC, Antoun N, et al. Imaging atherosclerotic plaque inflammation with [18F]-fluorodeoxyglucose positron emission tomography. Circulation 2002;105:2708-11.
9. Rudd JH, Myers KS, Bansilal S, Machac J, Woodward M, Fuster V, et al. Relationships among regional arterial inflammation, calcification, risk factors, and biomarkers: A prospective fluorodeoxyglucose

positron-emission tomography/computed tomography imaging study. Circ Cardiovasc Imaging 2009;2:107-15.
10. Tatsumi M, Cohade C, Nakamoto Y, Wahl RL. Fluorodeoxyglucose uptake in the aortic wall at PET/CT: Possible finding for active atherosclerosis. Radiology 2003;229:831-7.
11. Tawakol A, Migrino RQ, Hoffmann U, Abbara S, Houser S, Gewirtz H, et al. Noninvasive in vivo measurement of vascular inflammation with F-18 fluorodeoxyglucose positron emission tomography. J Nucl Cardiol 2005;12:294-301.
12. Davies JR, Rudd JH, Fryer TD, Graves MJ, Clark JC, Kirkpatrick PJ, et al. Identification of culprit lesions after transient ischemic attack by combined 18F fluorodeoxyglucose positron-emission tomography and high-resolution magnetic resonance imaging. Stroke 2005;36:2642-7.
13. Meerwaldt R, Slart RH, van Dam GM, Luijckx GJ, Tio RA, Zeebregts CJ. PET/SPECT imaging: From carotid vulnerability to brain viability. Eur J Radiol 2010;74:104-9.
14. Okane K, Ibaraki M, Toyoshima H, Sugawara S, Takahashi K, Miura S, et al. 18F-FDG accumulation in atherosclerosis: Use of CT and MR co-registration of thoracic and carotid arteries. Eur J Nucl Med Mol Imaging 2006;33:589-94.
15. Rominger A, Saam T, Wolpers S, Cyran CC, Schmidt M, Foerster S, et al. 18F-FDG PET/CT identifies patients at risk for future vascular events in an otherwise asymptomatic cohort with neoplastic disease. J Nucl Med 2009;50:1611-20.
16. Tahara N, Kai H, Yamagishi S, Mizoguchi M, Nakaura H, Ishibashi M, et al. Vascular inflammation evaluated by [18F]-fluorodeoxyglucose positron emission tomography is associated with the metabolic syndrome. J Am Coll Cardiol 2007;49:1533-9.
17. Tahara N, Kai H, Nakaura H, Mizoguchi M, Ishibashi M, Kaida H, et al. The prevalence of inflammation in carotid atherosclerosis: Analysis with fluorodeoxyglucose-positron emission tomography. Eur Heart J 2007;28:2243-8.
18. Tai YC, Ruangma A, Rowland D, Siegel S, Newport DF, Chow PL, et al. Performance evaluation of the microPET focus: A third-generation microPET scanner dedicated to animal imaging. J Nucl Med 2005;46:455-63.
19. Graebe M, Pedersen SF, Borgwardt L, Hojgaard L, Sillesen H, Kjaer A. Molecular pathology in vulnerable carotid plaques: Correlation with [18]-fluorodeoxyglucose positron emission tomography (FDG-PET). Eur J Vasc Endovasc Surg 2009;37:714-21.
20. Sheikine Y, Akram K. FDG-PET imaging of atherosclerosis: Do we know what we see? Atherosclerosis 2010;211:371-80.
21. North American Symptomatic Carotid Endarterectomy Trial Collaborators. Beneficial effect of carotid endarterectomy in symptomatic patients with high-grade carotid stenosis. N Engl J Med 1991;325:445-53.
22. European Carotid Surgery Trialists' Collaborative Group. Randomised trial of endarterectomy for recently symptomatic carotid stenosis: Final results of the MRC European Carotid Surgery Trial (ECST). Lancet 1998;351(9113):1379-87.
23. Becker CR, Kleffel T, Crispin A, Knez A, Young J, Schoepf UJ, et al. Coronary artery calcium measurement: Agreement of multirow detector and electron beam CT. AJR Am J Roentgenol 2001;176:1295-8.
24. Hamacher K, Coenen HH, Stocklin G. Efficient stereospecific synthesis of no-carrier-added 2-[18F]-fluoro-2-deoxy-D-glucose using aminopolyether supported nucleophilic substitution. J Nucl Med 1986;27:235-8.
25. Hellings WE, Pasterkamp G, Vollebregt A, Seldenrijk CA, de Vries JP, Velema E, et al. Intraobserver and interobserver variability and spatial differences in histologic examination of carotid endarterectomy specimens. J Vasc Surg 2007;46:1147-54.

26. Rudd JH, Narula J, Strauss HW, Virmani R, Machac J, Klimas M, et al. Imaging atherosclerotic plaque inflammation by fluorode-oxyglucose with positron emission tomography: Ready for prime time? J Am Coll Cardiol 2010;55:2527-35.

27. Graebe M, Pedersen SF, Hojgaard L, Kjaer A, Sillesen H. 18FDG PET and ultrasound echolucency in carotid artery plaques. JACC Cardiovasc Imaging 2010;3:289-95.

28. Davies JR, Izquierdo-Garcia D, Rudd JH, Figg N, Richards HK, Bird JL, et al. FDG-PET can distinguish inflamed from non-inflamed plaque in an animal model of atherosclerosis. Int J Cardiovasc Imaging 2010;26:41-8.

29. Calder PC, Dimitriadis G, Newsholme P. Glucose metabolism in lymphoid and inflammatory cells and tissues. Curr Opin Clin Nutr Metab Care 2007;10:531-40.

30. Kietselaer BL, Reutelingsperger CP, Heidendal GA, Daemen MJ, Mess WH, Hofstra L, et al. Noninvasive detection of plaque instability with use of radiolabeled annexin A5 in patients with carotid-artery atherosclerosis. N Engl J Med 2004;350:1472-3.

31. Font MA, Fernandez A, Carvajal A, Gamez C, Badimon L, Slevin M, et al. Imaging of early inflammation in low-to-moderate carotid stenosis by 18-FDG-PET. Front Biosci 2009;14:3352-60.

32. Tawakol A, Migrino RQ, Bashian GG, Bedri S, Vermylen D, Cury RC, et al. In vivo 18F-fluorodeoxyglucose positron emission tomography imaging provides a noninvasive measure of carotid plaque inflammation in patients. J Am Coll Cardiol 2006;48:1818-24.

33. Ben-Haim S, Kupzov E, Tamir A, Israel O. Evaluation of 18F-FDG uptake and arterial wall calcifications using 18F-FDG PET/CT. J Nucl Med 2004;45:1816-21.

34. Dunphy MP, Freiman A, Larson SM, Strauss HW. Association of vascular 18F-FDG uptake with vascular calcification. J Nucl Med 2005;46:1278-84.

35. Kwee RM, van Oostenbrugge RJ, Hofstra L, Teule GJ, van Engelshoven JM, Mess WH, et al. Identifying vulnerable carotid plaques by noninvasive imaging. Neurology 2008;70:2401-9.

36. Laitinen I, Marjamaki P, Haaparanta M, Savisto N, Laine VJ, Soini SL, et al. Non-specific binding of [18F]FDG to calcifications in atherosclerotic plaques: Experimental study of mouse and human arteries. Eur J Nucl Med Mol Imaging 2006;33:1461-7.

37. Silvera SS, Aidi HE, Rudd JH, Mani V, Yang L, Farkouh M, et al. Multimodality imaging of atherosclerotic plaque activity and composition using FDG-PET/CT and MRI in carotid and femoral arteries. Atherosclerosis 2009;207:139-43.

38. Williams G, Kolodny GM. Retrospective study of coronary uptake of 18F-fluorodeoxyglucose in association with calcification and coronary artery disease: A preliminary study. Nucl Med Commun 2009;30:287-91.

39. Ben-Haim S, Kupzov E, Tamir A, Frenkel A, Israel O. Changing patterns of abnormal vascular wall F-18 fluorodeoxyglucose uptake on follow-up PET/CT studies. J Nucl Cardiol 2006;13:791-800.

40. Paulmier B, Duet M, Khayat R, Pierquet-Ghazzar N, Laissy JP, Maunoury C, et al. Arterial wall uptake of fluorodeoxyglucose on PET imaging in stable cancer disease patients indicates higher risk for cardiovascular events. J Nucl Cardiol 2008;15:209-17.